Polyhedron 50 (2013) 306–313

Contents lists available at SciVerse ScienceDirect

Polyhedron

journal homepage: www.elsevier.com/locate/poly

Complexes of Zn(II) containing (o-)/(p-) carboxylato phenyl azo pentane 2,4-dione and 2,2′ bipyridine as ligands: Synthesis, characterization, colorimetric and fluorometric modulation in the presence of Ag^+ ions

Md. Amin Hasan, Niraj Kumari, Pankaj Kumar, Brajesh Pathak, Lallan Mishra *

Department of Chemistry, Faculty of Science, Banaras Hindu University, Varanasi 221 005, India

ARTICLE INFO

Article history:
Received 5 October 2012
Accepted 2 November 2012
Available online 20 November 2012

Keywords:
Azodiketone
Zn(II) complex
X-ray diffraction
Spectral titration
Switching of optical signal

ABSTRACT

Azo–enol based ligands 2-[N′-(1-acetyl-2-oxo-propylidene) hydrazino]-benzoic acid (L_1H_2) and 4-[N′-(1 acetyl-2 oxo-propylidene)-hydrazino]-benzoic acid (L_2H_2) and their complexes $[Zn(L_1H)_2(bpy)]$ (**1**) and $[Zn(L_2H)_2(bpy)]$ (**2**) (where bpy = 2, 2′-bipyridine) have been synthesized and characterized using elemental analyses, spectral (FT-IR, ^1H NMR, ^{13}C NMR, electronic absorption), emission and single-crystal X-ray diffraction studies. Complexes **1** and **2** display selective chromogenic and fluorogenic responses with Ag^+ ions in the presence of several other metal ions. The binding is monitored separately using UV–Vis, fluorescence and ^1H NMR spectral titrations. Job's plot supports a 1:2 stoichiometry for **1** and **2** with Ag^+ ions. The pH dependent "on–off" switching of fluorescence from complexes **1** and **2** have been studied. The fluorescence intensity quenches (turns-off) upon addition of OH^- ions, while it enhances (turns-on) in the presence of H^+ ions.

1. Introduction

A display of host–guest chemistry leading the synthesis of new chemosensors and their exploitation in guest binding, monitored by the changes in optical signals specially fluorescence, has been a vibrant area of research [1–7]. Chemosensors targeting heavy transition metal (HTM) ions are very important owing to their environmental and biological relevance [8]. Sensors based on organic chromophores, [9–12] redox potentials [13] and nanomaterials [14,15] have also been developed for the detection of different types of analytes. In view of the sensitivity, selectivity and simplicity, the exploration of systems, especially for the recognition of metal ions, have some limitations. The known reversible chemosensors generally work well in organic and/or aqueous or mixed organic co-solvent mediums, and some of them work efficiently under strong acidic or alkaline conditions [9,16,17].

Fluorescence based sensors for the detection of metal ions such as Hg(II), Pb(II), Ag(I) and Cu(II) are challenging to find since these ions generally act as quenchers via electron transfer and facilitate intersystem crossing (isc) processes. However, several chemosensors for the detection of these ions have been reported [18,19] and most of them display changes in fluorescence intensity. In this context, it was observed that photoinduced electron and proton transfers are fundamental processes and are generally exhibited by a number of natural systems, including azo–enol systems. It was also found that silver complexes have been exploited in medicine and agriculture, and their prolonged use leads to irreversible darkening of the skin and mucous membrane [20]. Therefore selective and sensitive fluorescent sensors for the detection of Ag^+ ions demands more research in this area. In recent years, chemosensors bearing polyamine chains as receptor units [21,22] have been developed and after deprotonation they bind with cations, bringing about significant changes in their fluorescence. This favourable situation permits the use of electrostatic interactions and in some cases hydrogen bonding as a driving force for the binding of cations. In general, polyamines quench the emission from aromatic signalling units by photoinduced electron transfer (PET) processes. However, coordination of amines to metal ions like Zn(II) and Cd(II) prevents the quenching mechanism and allows the emission of the signalling unit to appear [23–27]. In some receptor units, aromatic nitrogen heterocycles, like pyridine, have been integrated into the ligand to modulate its binding properties. In such cases, protonation of the aromatic nitrogen at acidic pH gives rise to PET from the excited fluorophore to the protonated heterocycle, resulting in fluorescence quenching [26,27]. Systems containing both aliphatic amines and nitrogen heterocycles are effective only in a pH window whose width is dependent on the structure of the molecule. Thus, it was thought that detection of the metal ions of choice using an entirely different class of materials could be a worthy target in this highly competitive area of research.

* Corresponding author. Tel.: +91 542 6702449; fax: +91 542 2368174.
E-mail address: lmishrabhu@yahoo.co.in (L. Mishra).

0277-5387/$ - see front matter © 2012 Elsevier Ltd. All rights reserved.
http://dx.doi.org/10.1016/j.poly.2012.11.012

2. Experimental

2.1. Materials and methods

Reagents of A.R. grade were purchased from Sigma–Aldrich and Merck, and were used without further purification. Solvents were dried and distilled using standard procedures [28]. Elemental analysis was carried out using a Carbo-Erba elemental analyzer 1108, IR spectra were recorded as KBr pellets using a Varian 3100 FT-IR spectrometer and ^{1}H NMR spectra were recorded on a JEOL AL 300 MHz spectrometer using DMSO-d_6 as the solvent and TMS as an internal reference. A Shimadzu UV-1701 spectrophotometer was used to record UV–Vis spectra and emission spectra were recorded in Tris–HCl buffer [pH 7–8; (DMSO/water 1:9; v/v)] at room temperature using a Shimadzu UV-1601 spectrometer and a Perkin Elmer LS-45 luminescence spectrometer. The time-resolved fluorescence delay was measured on a single-photon counting spectrometer equipped with pulsed nanosecond LED excitation heads at 280 nm (HORIBA, Jobin Yvon, IBH Ltd., Glasgow, UK), run in reverse mode. This experiment was also performed at room temperature. The fluorescence lifetime data were measured to 10 000 counts in the peak, unless otherwise indicated. The instrumental response function was recorded sequentially using a scattering solution and a time calibration of 114 ps/channel. Data were analyzed by using a sum of exponentials, employing a non-linear least squares reconvolution analysis from HORIBA, Jobin Yvon, IBH Ltd. The pH values of the solutions were measured on a CyberScan pH/mV/°C/F metre with MFRS (Toshniwal Instruments, MFG Pvt. Ltd.), using the reported method [29]. Stock solution (25 mL) of the complexes (1×10^{-3} M) were prepared initially in DMSO as they were sparingly soluble in water. To 1.0 mL of the stock solutions of complexes in DMSO, 9.0 mL of 0.5 M aqueous HCl was added to get a 10 mL stock solutions of 1×10^{-4} M concentration. The pH of the solution was varied between 2 and 12 by the addition of a calculated amount of aqueous 1.0 M NaOH solution (~10 μL), consequently forming a B/BH$^+$ type buffer system. The solution was stirred for 3–5 min and the pH was recorded with the help of a digital pre-calibrated pH metre, and then absorption and luminescence spectra were measured at a particular pH. For a typical titration experiment, the stock solutions of **1** and **2** (1.0×10^{-5} M) were prepared separately using spectroscopic grade DMSO and triply distilled H_2O (1:9, v/v) in 0.01 M Tris–HCl buffer. The solutions of nitrate salts of Li^+, Na^+, K^+, Ca^{2+}, Mg^{2+}, Ag^+, Cu^{2+}, Fe^{3+}, Hg^{2+}, Ni^{2+}, Co^{2+} and Zn^{2+} were prepared by dissolving them in distilled water (5×10^{-4} M). Solutions (2.0 mL) of complexes **1** and **2** (1.0×10^{-5} M) were taken separately in a quartz cell of 10 mm path length, then the solutions of the metal ions were added (0–2.0 equiv) gradually in the cell. The spectra were recorded after equilibration for 5 min, allowing the complexes to bind with the cations. The absorption, if any, by the cations (guest molecules) was eliminated initially by keeping their equal quantities separately in the hosts (**1** and **2**) and a reference solution. From the absorption data, the intrinsic association constant K_a was determined from a plot of [guest]/($\varepsilon_a - \varepsilon_f$) versus [guest] using [30] Eq. (1)

$$[\text{guest}]/(\varepsilon_a - \varepsilon_f) = [\text{guest}]/(\varepsilon_b - \varepsilon_f) + [K_a(\varepsilon_b - \varepsilon_f)]^{-1}, \quad (1)$$

where [guest] are the metal ions to be detected. The apparent absorption coefficients ε_a, ε_f and ε_b correspond to A_{obsd}/[1] or A_{obsd}/[2], the extinction coefficient of the free **1** or **2** and the extinction coefficient of **1** or **2** in the fully bound form, respectively. The value of K_a (association constant) is given by the ratio of the slope to the intercept. The binding constants were calculated in duplicate, and an average is reported. For the fluorescence measurements, solutions of **1** and **2** (1.0×10^{-4} M) separately, together with the solutions of the cations to be detected (5×10^{-3} M), were prepared similarly as prepared for their titrations using absorption measurements. Luminescence titrations were performed by maintaining the concentration of the host molecules (**1** and **2**) at 10^{-4} M while the concentrations of the guest molecules (cations to be detected) were varied within (0–200)$\times 10^{-6}$ M, and the fluorescence spectra were measured until the fluorescence intensity reached a maximum. The fluorescence intensity was measured at λ_{ex} 370 nm. The maximum emission was observed at λ_{em} 458 and 459 nm for complexes **1** and **2**, respectively.

2.2. Synthesis of the ligands

The ligands L_1H_2 [31] and L_2H_2 [32] were synthesized and characterized by the reported methods. A solution of the diazonium salt was prepared under cooling (0–5 °C) from the respective aniline (20 mmol) in hydrochloric acid (3 N, 40 mL) and a conc. aqueous solution of sodium nitrite (1.37 g, 20 mmol), according to the standard procedure [33]. A cold solution of the diazonium salt was added under cooling (0 °C) and stirring to a mixture composed of pentane-2,4-dione (2.1 mL, 2.04 g, 20 mmol), sodium acetate (8.2 g, 100 mmol), methanol (160 mL) and water (160 mL). The mixture was then warmed to room temperature and stirred for 1 h. The corresponding precipitate was collected, washed with water and recrystallized from ethanol. The details for each compound are given below.

2.2.1. Synthesis of L_1H_2

2-Aminobenzoic acid (2.74 g, 20 mmol) was used for the synthesis of L_1H_2 and provided 3.9 g (78%) as a yellow powder, soluble in DMSO, methanol, ethanol and acetone, but insoluble in water. M.p.: 245 °C. *Anal.* Calc. for [$C_{12}H_{12}N_2O_4$]: C, 58.06; H, 4.87; N, 11.29. Found: C, 57.93; H, 5.03; N, 11.27%. IR (KBr pellets, cm^{-1}): 3482 ν(NH), 1680ν(C=O), 1633 ν(C=O), 1605 (C=O--H), 1518 ν(C=N), ^{1}H NMR (DMSO-d_6, 300 MHz, ppm) δ: 15.103 (s, 1H, –COOH), 13.707 (s, 1H, –NH), 7.983 (d, 2H, –Ph), 7.653 (d, 2H, –Ph), 2.510 (s, 3H, –CH$_3$), 2.483 (s, 3H, –CH$_3$). ^{13}C NMR (DMSOd$_6$, ppm) δ: 195.324 (C=O), 193.626 (C=O), 166.831 (COOH), 145.411 (C=N), 134.846 (Ph–H), 130.964 (Ph–H), 126.934 (Ar–H), 115.750 (Ph–C–COOH), 31.267 (CH$_3$), 26.338 (CH$_3$).

2.2.2. Synthesis of L_2H_2

4-Aminobenzoic acid (2.74 g, 20 mmol) was used in the synthesis and gave 3.75 g (75%) of L_2H_2 as a yellow powder. M.p.: 216–218 °C. *Anal.* Calc. for [$C_{12}H_{12}N_2O_4$]: C, 58.06; H, 4.87; N, 11.29. Found: C, 57.73; H, 4.93; N, 11.09%. IR (KBr pellets, cm^{-1}): 3451 ν(NH), 1680 ν(C=O), 1633 ν(C=O), 1605 (C=O--H), 1514 ν(C=N). ^{1}H NMR (DMSO-d_6, 300 MHz, ppm) δ: 15.201 (s, 1H, –COOH), 13.692 (s, 1H, –NH), 7.962 (d, 2H, J = 9.0 Hz, –Ph), 7.630 (d, 2H, J = 9.0 Hz, –Ph), 2.483 (s, 3H, –CH$_3$), 2.441 (s, 3H, –CH$_3$). ^{13}C NMR (DMSOd$_6$, ppm) δ: 194.337 (C=O), δ: 193.574 (C=O), 166.160 (COOH), 144.867 (C=N), 134.623 (Ph–C), 130.881 (Ph–C), 115.651 (Ph–C), 31.308 (CH$_3$), 26.437 (CH$_3$).

2.3. Synthesis of [Zn(L_1H)$_2$(bpy)] **1**

A solution of Zn(bpy)(NO$_3$)$_2$·2H$_2$O (0.363 g, 1 mmol) [34] dissolved in EtOH:DMF (3:1) (8 mL) was added dropwise to a solution of L_1H_2 (0.496 g, 2.0 mmol) in EtOH:DMF (3:1) (16 mL) over half an hour at 50 °C with stirring. The mixture was then heated under reflux for 18 h. After cooling to room temperature, it gave a yellow solid. This solid was recrystallized from EtOH/DMF (4:1), giving yellow crystals. Yield: 0.801 g (57%). M.p.: > 280 °C. *Anal.* Calc. for [$C_{34}H_{30}N_6O_8Zn$]: C, 57.03; H, 4.22; N, 11.74. Found: C, 57.10; H, 4.11; N, 11.45%. IR (KBr pellets, cm^{-1}): 3430(w), 1686(vs), 1606(vs), 1524(s), 1383(vs), 1317(s), 1261(s), 1202(m), 1027(w),

931(w), 770(s), 659(vw). ^{1}H NMR (DMSO-d_6, 300 MHz, ppm) δ: 13.870 (s, 2H, –NH), 8.770 (s, 2H, bpy), 8.524 (s, 2H, bpy), 7.963 (d, J = 8.4 Hz, 8H, –Ph), 7.563 (d, J = 8.4 Hz, 4H, bpy), 2.490 (s, 6H, –CH_3), 2.456 (s, 6H, –CH_3). ^{13}C NMR (DMSOd_6, ppm) δ: 195.940 (C=O), 193.912 (C=O), 170.605 (COOH), 166.114 (bpy), 165.718 (bpy), 152.779 (bpy), 149.730 (bpy), 141.410 (C=N), 149.112 (bpy), 131.046 (Ph–C), 130.000 (Ph–C), 129.151 (Ph–C), 122.673 (Ph–C), 121.544 (Ph–C), 114.085 (Ph–C), 113.719 (Ph–C), 30.632 (CH_3), 28.489 (CH_3). UV–Vis (DMSO:H_2O = 1:9, 10^{-5} M) λ_{max} (nm) ($\varepsilon_{max} \times 10^5$ M^{-1} cm^{-1}): 372 (0.19284). Emission at λ_{ex} 370 nm (DMSO:H_2O = 1:9, 10^{-4} M) λ_{max}(nm) (intensity in a.u.): 458 (10.5).

2.4. Synthesis of [Zn(L_2H)$_2$(bpy)] **2**

Using a procedure similar to that adopted for the synthesis of **1**, a solution of Zn(bpy)$(NO_3)_2\cdot 2H_2O$ (0.363 g,1 mmol) in EtOH:DMF (3:1) (8 mL) was added dropwise to a solution of L_2H_2 (0.496 g, 2.0 mmol) in EtOH:DMF (3:1) (16 mL) with stirring at 50 °C over half an hour. The mixture was then refluxed for 18 h. After cooling to room temperature it gave a yellow solid which was recrystallized from EtOH/DMF (4:1) as yellow crystals. Yield: 0.950 g (68%). M.p. > 280 °C. *Anal.* Calc. for [$C_{34}H_{30}N_6O_8Zn$]: C, 57.03; H, 4.22; N, 11.74. Found: C, 57.80; H, 4.01; N, 11.28%. IR (KBr pellets, cm^{-1}): 3437(w), 1686(vs), 1608(vs), 1525(s), 1443(s), 1375(s), 1353(vs), 1317(s), 1202(s), 1161(m), 1028(w), 837(vw), 771(s), 453(w). ^{1}H NMR (DMSO-d_6, 300 MHz, ppm) δ: 13.878 (s, 2H, –NH), 8.788 (s, 2H, –bpy), 8.549 (s, 2H, bpy), 7.949 (d, J = 7.8 Hz, 4H, –Ar), 7.570 (d, J = 7.5 Hz, 4H, –Ar), 7.544 (d, J = 10.5 Hz, 4H, bpy), 2.490 (s, 6H; –CH_3), 2.416 (s, 6H; –CH_3). ^{13}C NMR (DMSOd_6, ppm): δ: 194.575 (C=O), 192.819 (C=O), 172.932 (COOH), 151.677 (bpy), 148.899 (bpy), 148.619 (bpy), 148.446 (bpy), 146.081 (C=N), 131.378 (Ph–C), 128.386 (Ph–C), 127.158 (Ph–C), 123.639 (Ph–C), 121.084 (Ph–C), 114.111 (Ph–C), 110.469 (Ph–C), 31.036 (CH_3), 27.879 (CH_3). UV–Vis (DMSO:H_2O = 1:9, 10^{-5} M) λ_{max} (nm) ($\varepsilon_{max} \times 10^5$ M^{-1} cm^{-1}): 370 (0.237). Emission at λ_{ex} 370 nm (DMSO:H_2O = 1:9, 10^{-4} M) λ_{max} (nm) (intensity in a.u.): 459 (5.4).

2.5. X-ray Crystallographic Studies

Crystals of the complexes suitable for X-ray diffraction measurement were grown by layering solutions of the complexes in DMF with ethanol at room temperature. X-ray diffraction data were collected using an Oxford diffraction XCALIBUR-EOS diffractometer by mounting a single-crystal of the sample on a glass fibre. Appropriate empirical absorption corrections using the multi-scan programs were applied. Monochromated Mo Kα radiation (λ = 0.71073 Å) was used for the measurements. The crystal structures were solved by direct methods using the SHELXS-97 program [35] and have been refined by full matrix least squares, SHELXL-97 [36]. Drawings were carried out using MERCURY [37] and special computations were carried out using PLATON [38].

3. Result and discussion

The ligands L_1H_2 and L_2H_2 were synthesized and characterized by the reported methods. These ligands were reacted separately with [Zn(bpy)$(NO_3)_2\cdot 2H_2O$] to afford mononuclear complexes **1** and **2** in reasonably good yields (S1). Complexes **1** and **2** were characterized by analytical, spectral (IR, NMR, UV–Vis, emission) techniques. The structures of **1** and **2** were authenticated by their single crystal X-ray diffraction analyses.

In the infrared spectra of complexes **1** and **2**, the ν(COO) vibration of the ligands L_1H_2 (1516 cm^{-1}) and L_2H_2 (1514 cm^{-1}) shifted to a higher position by 8–11 cm^{-1}. This indicates that the carboxylate groups in the ligands have coordinated to the Zn(II) ion [39]. The peaks appearing at ~1686 and 1607 cm^{-1} in the spectra of complexes **1** and **2**, respectively were assigned to an uncoordinated carbonyl stretching vibration. The bands observed at ~3400 to ~3200 cm^{-1} were assigned to υ(NH) vibrations. The –COOH protons observed at δ 15.2 ppm in the ^{1}H NMR spectra of ligands disappeared in the spectra of the corresponding complexes **1** and **2** (S2, S3). This supports that the deprotonated –COOH group has coordinated with the metal ion. The peak observed at δ 13.7 ppm in the spectrum of L_1H_2, assigned to NH protons, is shifted downfield to δ 13.8 ppm in the spectrum of complex **1** as a consequence of the coordination of its neighbouring –COO^- group and also owing to π-electron delocalization within a so-called "resonance assisted hydrogen bond" (RAHB) [40–44]. Phenyl protons were observed at δ 7.54–7.57 and 6.94–7.96 ppm as multiplets. Two methyl protons were observed as separate singlets at δ 2.490 and 2.456 ppm in the spectrum of complex **1** and at δ 2.490 and 2.416 ppm in the spectrum of complex **2**. The non-equivalent two methyl carbon atoms of the pentane-2,4-dione part of the complexes were also observed in their ^{13}C NMR spectra at room temperature (S4, S5). Two peaks observed at δ 30.632 and 28.489 ppm in the spectrum of complex **1** and at δ 31.036 and 27.879 ppm in the spectrum of complex **2** were assigned to the methyl carbon atoms. The peaks observed at δ 195.950 and 193.912 ppm in the spectrum of complex **1** and at δ 194.575 and 192.819 ppm in the spectrum of complex **2** were assigned to two different carbonyl carbon (C=O) atoms of the complexes. The –COOH carbon signals observed at δ 166.831 and 166.160 ppm in the spectra of the ligands L_1H_2 and L_2H_2 shifted to δ 170.605 and 172.932 ppm in the spectra of the corresponding complexes **1** and **2**, respectively. The UV–Vis electronic absorption spectra of L_1H_2 and L_2H_2 (DMSO/H_2O, 1:9, v/v) displayed intense bands at λ_{max} 364 and 369 nm (ε_{max} = 221600 and 180502 M^{-1} cm^{-1}, respectively). The bands were assigned to ligand-centred π–π* transitions. The spectra of complexes **1** and **2** recorded in the same solvents composition (DMSO/H_2O, 1:9, v/v), appeared at λ_{max} 372 nm (ε_{max} = 19284 M^{-1} cm^{-1}) and 370 nm (ε_{max} = 23702 M^{-1} cm^{-1}), as shown in Fig. 1(a).

3.1. Luminescence spectra

The emissions observed from the ligands and complexes were studied at room temperature (S6). The free ligands L_1H_2 and L_2H_2 displayed significant fluorescence at λ_{em} 424 (39.8 a.u.) and λ_{em} 424.7 nm (45.1 a.u.) on excitation at λ_{ex} 370 nm. However, their complexes **1** and **2** displayed only weak fluorescence at λ_{em} 458 (10.5 a.u.) and λ_{em} 457 nm (5.4 a.u.). The weaker emission displayed from the complexes probably occurs due to a reverse-PET effect owing to the transfer of electron density from the azodiketone unit to the coordinated carboxyl unit, in view of an earlier report [45]. However, this surmise calls for deeper investigation. The luminescence lifetime (τ) of the emission from complexes **1** and **2** of 235 and 237 ns, respectively was measured following excitation at (λ_{ex}) 370 nm and fitted with a mono-exponential decay (S7).

3.2. pH responsive optical signals

The emission peaks obtained from the ligands and the complexes were found to be pH-dependent. This could be attributed to the variation of the protonation/deprotonation equilibria of the respective ligands and complexes in DMSO/water (1:9, v/v). pH dependent UV–Vis spectrophotometric titrations were also carried out in the same solvent. The free ligands L_1H_2 and L_2H_2 showed peaks at λ_{max} 364 and 369 nm, respectively. On increasing the pH, the peaks intensified (S8). Complex **1** showed two peaks at λ_{max} 301 and 360 nm from pH 2–5 (S9). At pH 6.0, the former band

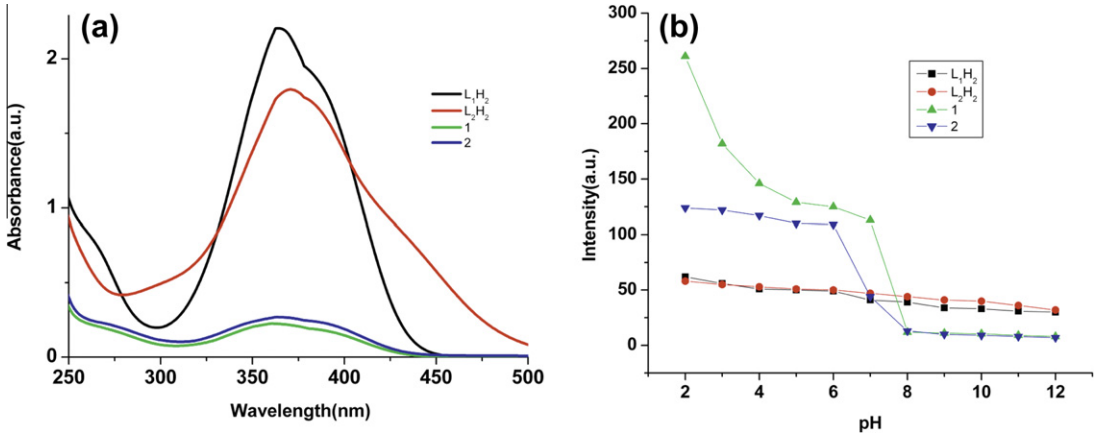

Fig. 1. (a) Absorption spectra of L_1H_2, L_2H_2, **1** and **2** in 0.01 M Tris HCl buffer (DMSO/H_2O, 1:9, v/v; pH ~ 7.0, $c = 1.0 \times 10^{-5}$ M); (b) Changes in the fluorescence intensity (I) of the ligands and complexes **1** and **2** with the variation of pH of the medium.

shifted to λ_{max} 285 nm, whereas the latter band shifted to λ_{max} 362 nm. Above pH 6, only one intense band was observed at λ_{max} 372 nm. The colour of complex **1** turned light green at pH 7.0, whilst at pH 8–12, the colour of the solution turned deep green. A similar pattern of pH dependent changes were also observed for complex **2** (S10). Such changes in colour and spectral wavelengths of the complexes could be attributed to restricted conjugation in acidic medium and enhanced conjugation in alkaline medium. The pH-dependent variations of the fluorescence from the ligands and complexes **1** and **2** are shown in Fig. 1(b). The emission intensities of complexes **1** and **2** are quenched to a larger extent at pH 7–8 (S11). However, at lower pH (~2), the emission was found to be maximum. Addition of H^+ ions (0.0–30.0 μL) to a solution of **1** over an interval of 5 min enhanced the fluorescence band 10-fold ("turn-on") together with a red shift from λ_{em} 456 to 461 nm. On the other hand, addition of OH^- (0.0–30.00 μL) to a solution of **1** over an interval of 5 min led to a 10-fold fluorescence quenching ("turn-off"), as depicted in Fig. 2. Similar fluorescence titrations using complex **2** also led to a 7-fold enhancement of the fluorescence and quenching upon addition of H^+ and OH^- ions, respectively (S12). The turn on and turn off behaviour of the fluorescence in acidic and neutral to alkaline medium could be understood in view of an earlier report [46]. Photo-induced intramolecular electron transfer or energy transfer from the deprotonated NH group to the diketone in neutral to alkaline medium is restricted owing to the protonation of the NH group in acidic medium (S13).

3.3. Structural description of the complexes

Structural refinement parameters of the complexes are given in Table 1. The selected bond distances (Å) and bond angles (deg) are shown in Table 2.

The molecular structure of complex **1**, together with the atom numbering scheme, is shown in Fig 3(a). It crystallized in the triclinic crystal system with the centrosymmetric space group $P\bar{1}$. There is one crystallographically independent Zn(II) ion and two L1 anions in the asymmetric unit. The Zn(II) centre is coordinated by two nitrogen atoms (N1 and N2) of 2,2′ bipyridine and four carboxylato O atoms (O1, O2, O5 and O6) of the ligand in a cis confugation with a Zn–O distance of 2.048(1)–2.515 Å in an octahedral geometry. The chelating 2,2′-bipyridine makes a bite angle of 78.75° (N1–Zn1–N2) and significantly contributes to the distortion of coordination geometry around the zinc(II) ion in **1**. The crystal structure showed strong intra molecular hydrogen bonding interactions [47] between N(3)···H(3N)---O(2), N(5)···H(5N)---O(5), N(5)···H(5N)---O(7) and N(3)···H(3N)·····O(4) at distances of 2.631, 2.643, 2.594 and 2.607 Å. The H-bonding interactions in complex **1** along the b axis provided an interesting double helical structure with a diameter of 9.115 Å. Two double helices are interconnected through a channel with a width of 8.134 Å (S14).

In contrast to the crystal pattern of complex **1**, complex **2** crystallized in the monoclinic crystal system with the space group $P12/c1$. There is one crystallographically independent Zn(II) ion and two L_2 anions in the asymmetric unit, in which Zn2 lies on a 2-fold

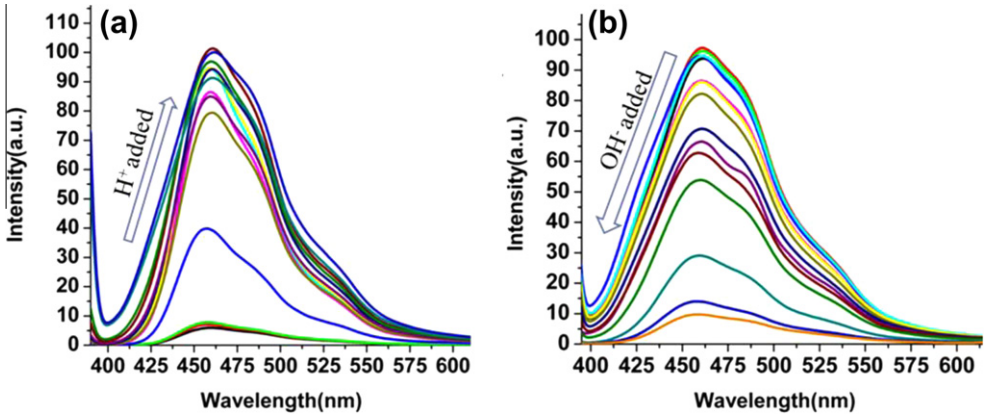

Fig. 2. Changes in fluorescence of complex **1** upon addition of H^+/OH^- ions.

Table 1
Selected crystallographic data of complexes **1** and **2**.

Parameters	1	2
Formula	$C_{34}H_{30}N_6O_8Zn$	$C_{34}H_{30}N_6O_8Zn$
M	716.01	716.01
Crystal system	triclinic	monoclinic
T (K)	120(2)	293(2)
Space group	$P\bar{1}$	$P1\ 2/c\ 1$
a (Å)	8.2527(5)	16.085(3)
b (Å)	12.6045(7)	7.9279(12)
c (Å)	15.6285(10)	13.452(3)
α (°)	79.649(5)	90
β (°)	85.520(5)	103.55(2)
γ (°)	85.864(5)	90
V (Å^3)	1591.55(17)	1667.7(5)
Z	2	2
D_c (Mg m^{-3})	1.494	1.426
Reflections collected/unique	11882/5539	13996/3951
Data/restraints/parameters	5539/0/454	3951/0/224
R_{int}	0.0471	0.1076
θ range for data collection (°)	2.89–25.00	3.00–29.18
Completeness to θ = 25.00	98.9	87.4
Final R indices [I > 2σ(I)]	R_1 = 0.0358, wR_2 = 0.0565	R_1 = 0.0700, wR_2 = 0.1033
R indices (all data)	R_1 = 0.0719, wR_2 = 0.0603	R_1 = 0.1575, wR_2 = 0.1307
Refinement method	Full-matrix, least-squares on F^2	
Goodness-of-fit (GOF)	0.770	1.297
Largest difference in peak and hole (e Å^{-3})	0.327 and −0.368	0.478 and −0.501

Table 2
Selected bond lengths (Å) and angles (deg) of complexes **1** and **2**, respectively.

1		2	
Zn(1)–O(5)	1.9784(18)	Zn(1)–N(4)	2.063(4)
Zn(1)–O(1)	2.048(2)	Zn(1)–O(1)	2.148(5)
Zn(1)–N(1)	2.070(2)	Zn(1)–O(1)#1	2.148(5)
Zn(1)–N(2)	2.0714(19)	Zn(1)–O(3)	2.262(5)
Zn(1)–O(2)	2.3067(17)	Zn(1)–O(3)#1	2.262(5)
Zn(1)–O(6)	2.515	N(4)#1–Zn(1)–N(4)	78.7(2)
O(5)–Zn(1)–O(1)	122.93(8)	N(4)–Zn(1)–O(1)	137.05(16)
O(1)–Zn(1)–N(1)	125.49(8)	O(1)–Zn(1)–O(1)#1	121.8(2)
O(5)–Zn(1)–N(2)	123.48(8)	N(4)#1–Zn(1)–O(3)	122.87(16)
O(1)–Zn(1)–N(2)	98.71(8)	N(4)–Zn(1)–O(3)	91.95(17)
N(1)–Zn(1)–N(2)	78.75(8)	O(1)–Zn(1)–O(3)	58.90(17)
O(5)–Zn(1)–O(2)	93.99(7)	O(1)#1–Zn(1)–O(3)	98.85(16)
O(1)–Zn(1)–O(2)	59.90(7)	N(4)–Zn(1)–O(3)#1	122.87(16)
N(1)–Zn(1)–O(2)	89.02(7)	O(1)–Zn(1)–O(3)#1	98.85(16)
N(2)–Zn(1)–O(2)	142.03(7)	O(3)–Zn(1)–O(3)#1	136.2(2

axis. Each Zn(II) is coordinated by four oxygen atoms from carboxylato groups of L_1H at a Zn–O distance of 2.148(5)–2.262(5)Å in a *cis* configuration, along with two bipyridyl nitrogen atoms (Zn–N = 2.063(4) Å) in an octahedral geometry, as shown in Fig. 3(b). Owing to the positional difference of the carboxylato group present in the skeleton of the ligand as compared to their positions in complex **1**, the crystal structure of complex **2** showed both intra as well as inter molecular hydrogen bonding interactions between N(3)···H(1)---O(6) and O(6)...H----O(6) at distances of 2.582 and 2.944 Å, respectively. The intermolecular hydrogen bonding interactions lead to a 1D- zigzag arrangement of the Zn(II) ions along the [1 0 1] axis (S15). Thus, the crystal structures of both complexes demonstrated diverse structural orientation owing to the presence of carboxylato groups in two different positions (ortho and para-) of the phenyl ring.

3.4. Ag^+ sensing by complexes 1 and 2

3.4.1. Colorimetric response of complexes *1* and *2* to Ag^+ ions

Owing to the presence of uncoordinated diketonic groups in the molecular structures of complexes **1** and **2**, it was thought worthwhile to exploit them as receptors for metal ions. The sensing abilities of **1** and **2** have been studied on a qualitative basis by visual examination of the Ag^+ induced colour changes in DMSO/H_2O (1:9, v/v) solutions (1×10^{-5} M) before and after addition the metal salts. As shown in Fig. 4, dramatic changes in the colour of **1** and **2** occurred on addition of 2.0 equivalents of Ag^+ ions separately to their solutions. In this context, solutions of **1** and **2** were prepared separately in DMSO/H_2O (1:9, v/v), then treated initially with several metal ions, namely Li^+, Na^+, K^+, Ca^{2+}, Mg^{2+}, Ag^+, Cu^{2+}, Fe^{3+}, Hg^{2+}, Ni^{2+}, $Co^{2+}$and Zn^{2+} (2.0 equiv. each). However, out of these metal ions, only addition of Ag^+ (2.0 equiv) separately to the solutions of **1** and **2** lead to "naked-eye" visible colour changes from yellow to light brown and from light yellow to pink, respectively. Addition of Fe^{3+} and Co^{2+} ions in the presence of complex **1** also brought about a slight change in the colour of the complex, but it could not be considered as a detectable colour change. However, to check the delayed response of the complex, if any, with a slow exchange cation like Fe^{3+}, spectra were recorded at different intervals of time, but no significant change in the spectra was observed even after one hour (S16). This observation called for better understanding of the affinity of **1** and **2** for Ag^+ ions. Ligands L_1H_2 and L_2H_2 did not show any colour change upon addition of cations (S17). The naked eye detection limit of Ag^+ is 25 μM in DMSO/H_2O (1:9, *v/v*) solution.

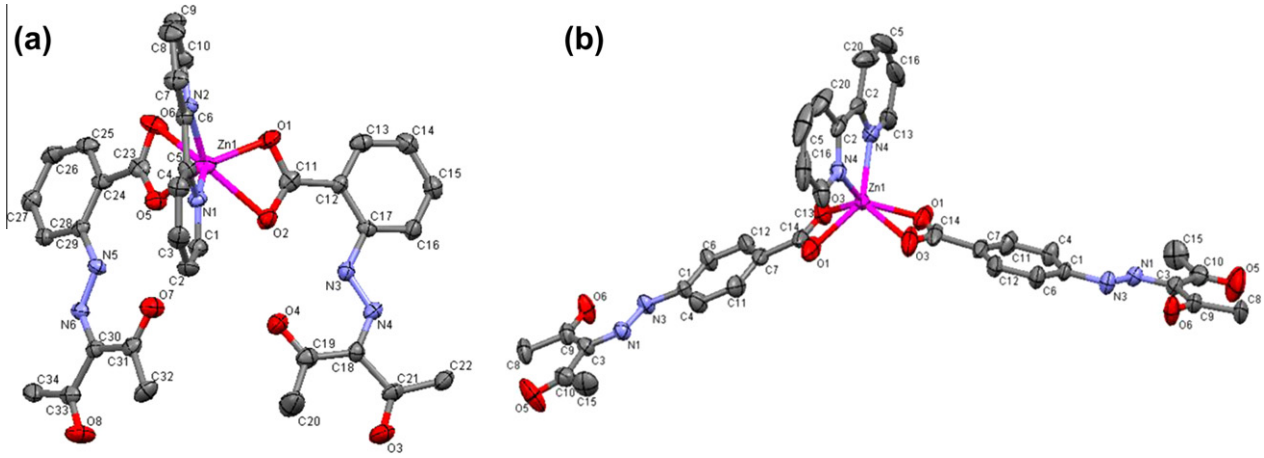

Fig. 3. Molecular structure of (a) complex **1** at 30% probability; (b) complex **2** at 30% probability; hydrogen atoms are omitted for clarity.

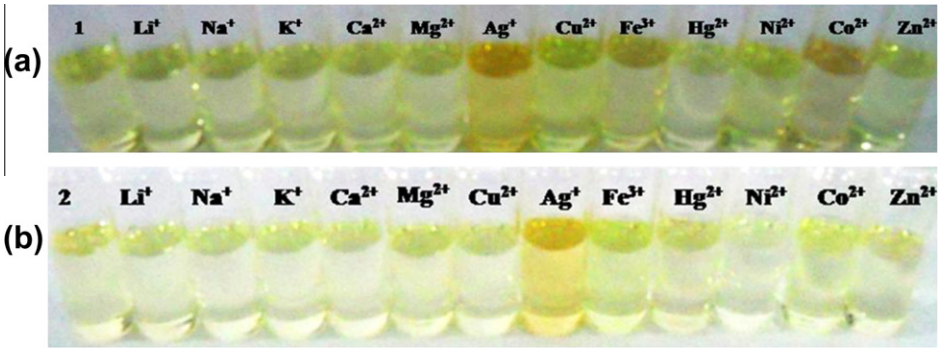

Fig. 4. Chromogenic changes observed for (a) complex **1** and (b) complex **2** in the presence of different metal ions in DMSO/H_2O (1:9, v/v) solution.

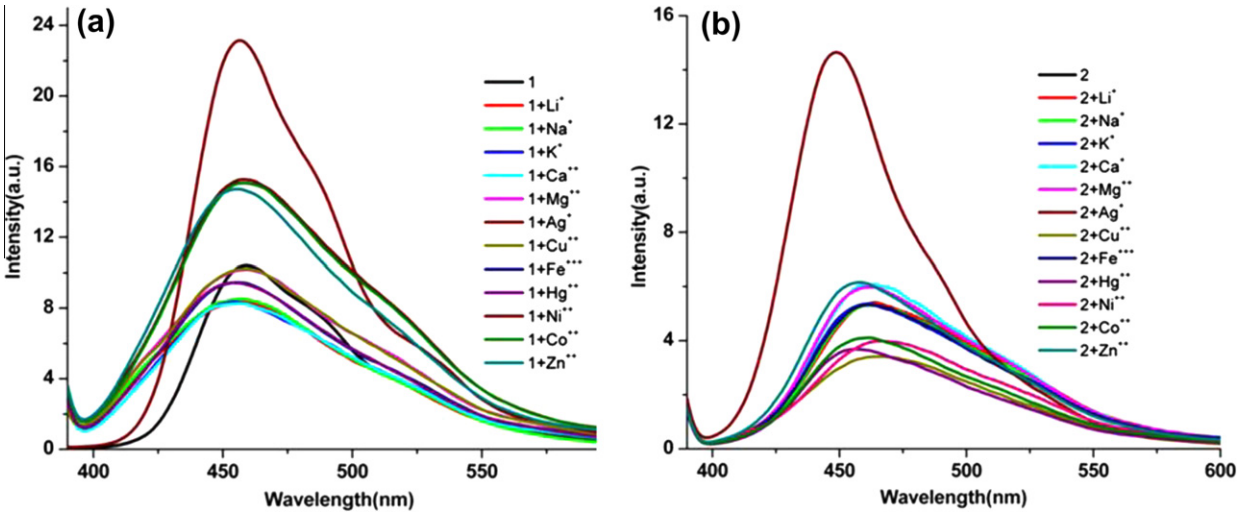

Fig. 5. Changes in emission spectra of complex **1** (a) and **2** (b) in DMSO/H_2O (1:9, v/v) solution upon addition of different cations.

3.4.2. Absorption spectral titrations

UV–Vis spectroscopy was employed to quantify the ion-induced spectral changes in **1** and **2**. The ligands L_1H_2 and L_2H_2 did not show any change upon addition of 10 equivalents of different metal cations (S18). The position of the MLCT bands at λ_{max} 372 and 370 nm for complexes **1** and **2**, respectively, remain practically unchanged upon addition of 10 equiv of Li^+, Na^+, K^+, Ca^{2+}, Mg^{2+}, Cu^{2+}, Fe^{3+}, Hg^{2+}, Ni^{2+}, $Co^{2+}$and Zn^{2+} (S19). On the other hand, the position of the MLCT band at λ_{max} 372 and 370 nm for complexes **1** and **2** shifted to λ_{max} 360 and 364 nm, respectively, on addition of 2.0 equivalent of Ag^+ ions (S19). It indicated strong interactions between the receptors and Ag^+ ions. These observations were in consonance with the visual changes already shown in Fig. 4. To obtain quantitative information about the receptor–ion interaction, spectrophotometric titrations of the receptors were carried out with Ag^+ ions. Absorption spectral titrations were performed by the addition of $AgNO_3$ (0.0–3.0 equiv, Tris–HCl buffer, DMSO/H_2O, 1:9, v/v, pH ~ 7.0) separately to solutions of **1** and **2** (S20). Incremental addition of Ag^+ ions to a solution of **1** (DMSO/H_2O, 1:9, v/v) showed that its original MLCT band, observed at λ_{max} 372 nm, shifted to λ_{max} 360 nm (ε_{max} = 23 888 M^{-1} cm^{-1}). Thus, it brought about a change in the colour of **1** from yellow to light brown. Under similar conditions, complex **2** also showed a blue-shift of its MLCT band by a $\Delta\lambda$ value of 6 nm (S20). These changes in the position of the MLCT transition could be attributed to coordination of Ag^+ ions, concomitantly reducing the conjugation in the ligand framework. A 1:2 stoichiometry between the complexes and Ag^+ ions was established using Job's method (S21) [48,49]. The values of association constants ($K_a = 8.77 \times 10^4\ M^{-1}$ for the Ag^+ ion with **1** and $K_a = 7.89 \times 10^4\ M^{-1}$ for the Ag^+ ion with **2**) suggested that the Ag^+ ion has a stronger binding affinity with **1** than **2**. A higher binding affinity of complex **1** as compared to **2** could be attributed to the changes in orientation of the corresponding ligand framework around the Zn(II) ion.

3.4.3. Fluorescence titrations

The ligands are fluorescent, but they did not cause any appreciable change after addition of metal cations (S22). Although the luminescence observed from both complexes was very weak, it demonstrated its potential to probe Ag^+ ions. As shown in Fig. 5, the emission intensity of the band observed at λ_{em} 458 nm from **1** and λ_{em} 459 nm from **2**, changed insignificantly on addition of two equivalents of Li^+, Na^+, K^+, Ca^{2+}, Mg^{2+}, Cu^{2+}, Fe^{3+}, Hg^{2+}, Ni^{2+}, $Co^{2+}$and Zn^{2+} ions. However, on addition of 2.0 equivalents of Ag^+ ions, the emission intensity of the band was significantly enhanced. The fluorescence enhancement was also accompanied by a blue shift of the emission band, observed at λ_{em} 455 nm for **1** and λ_{em} 449 nm for **2** (Fig. 5). Luminescence titrations of the complexes with Ag^+ ions have also been carried out (S23). The insets show the enhancement of luminescence intensities versus the concentration of added ions. These observations are consistent with those obtained from the absorption experiments. To investigate selective responses of both **1** and **2** to Ag^+ ions, variations of the luminescence spectra of complexes **1** and **2** in the presence of other related metal ions were also recorded. As shown in Fig. 6, only the addition of Ag^+ ions resulted in a significant enhancement in

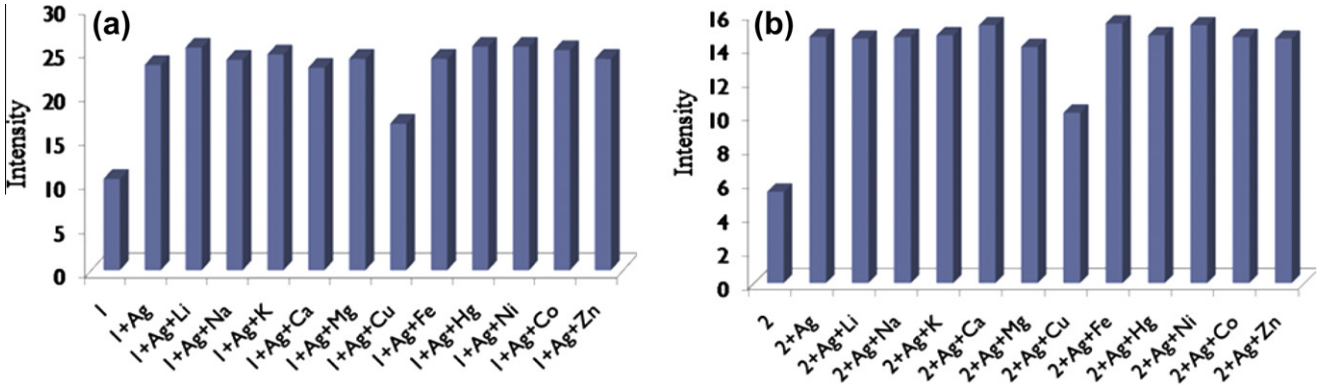

Fig. 6. Bar representation of the luminescent response of complexes **1** and **2** (100 μM) in the presence of various metal cations.

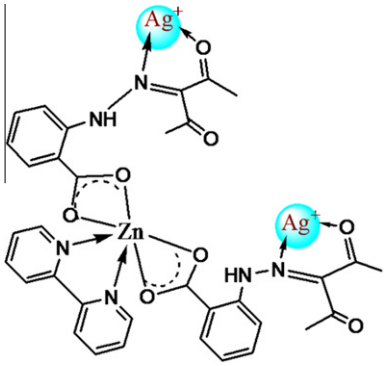

Fig. 7. Tentatively proposed mode of binding of complex **1** with Ag^+ ions.

luminescence from both complexes, whereas addition of a large excess of other competitive cations (such as Li^+, Na^+, K^+, Ca^{2+}, Mg^{2+}, Cu^{2+}, Fe^{3+}, Hg^{2+}, Ni^{2+}, Co^{2+} and Zn^{2+}) caused only slight luminescent changes. This supports that complexes **1** and **2** display a high selectivity for Ag^+ ions. No interference in luminescence was observed in the presence of competitive cations, as shown in Fig. 6.

3.4.4. NMR titrations

The ^{13}C NMR spectrum of a representative sample of complex **1** in the presence of 2.0 equivalents of Ag^+ ions was recorded and compared with the ^{13}C NMR spectrum of free complex **1** to explore the probable binding sites of the Ag^+ ions. In the spectrum of the free complex, out of two types of ›C═O carbon observed at δ 195.940 and 193.912 ppm, one ›C═O carbon was shifted to δ 196.425 ppm, whereas the other remained almost constant after addition of 2.0 equivalents of Ag^+ ions (S24). Thus, it supported that the Ag^+ ions are coordinated through only one ketonic ›C═O group. Another coordinating group could most likely be the –C═N group of complex **1** as its –C═N carbon, observed at δ 141.496 ppm, shifted to δ 141.974 ppm on complexation with the Ag^+ ions. It was also interesting to observe that in the spectrum of the Ag^+ bound complex, the phenyl and bipyridyl carbon atoms were also shifted as compared to their peak positions in the spectrum of free complex **1**. This type of change could be attributed to the heavy atom effect of the Ag^+ ion, which on coordination might bring about some rearrangements in the coordination positions of the ligands, especially the bipyridyl group which may occupy an axial position (Fig. 7) instead of its original equatorial position, as shown in Fig. 3(a).

4. Conclusions

The present manuscript embodies the synthesis and characterization of two mononuclear, octahedral Zn(II) complexes, $[Zn(L_1H)_2(bpy)]$ (**1**) and $[Zn(L_2H)_2(bpy)]$ (**2**), containing azo ligand frameworks, obtained by the coupling of diazonium salts of o-/p-carboxylato aniline separately to pentane 2,4-dione, henceforth abbreviated as L_1H_2 and L_2H_2, respectively. The crystal packing of complex **1**, using intramolecular H-bonding, provides an interesting framework of a double helical right handed DNA. One double helical structure is attached to another through a channel with a diameter of 8.134 Å. The difference in the supramolecular packing pattern of the two complexes is due to the difference in the orientation of their ligand frameworks around the central metal ion. Both complexes show pH dependent "on–off" switching of their fluorescence and bind selectively with 2.0 equivalents of Ag^+ ions. Their chromogenic and fluorogenic modulations are monitored using UV–Vis absorption, fluorescence and NMR titrations.

Acknowledgements

Financial support received from UGC (Grant No. F. No. 34-468/2008 to L.M.) and DST, New Delhi, India is gratefully acknowledged.

Appendix A. Supplementary data

CCDC 866469 and 866468 contain the supplementary crystallographic data for complexes **1** and **2**, respectively. These data can be obtained free of charge via http://www.ccdc.cam.ac.uk/conts/retrieving.html, or from the Cambridge Crystallographic Data Centre, 12 Union Road, Cambridge CB2 1EZ, UK; fax:+44 1223 336 033; or e-mail: deposit@ccdc.cam.ac.uk. Supplementary data associated with this article can be found, in the online version, at http://dx.doi.org/10.1016/j.poly.2012.11.012.

References

[1] G. He, Y. Zhao, C. He, Y. Liu, C. Duan, Inorg. Chem. 47 (2008) 5169.
[2] M.G. Choi, D.H. Ryu, H.L. Jeon, S. Cha, J. Cho, H.H. Joo, K.S. Hong, C. Lee, S. Ahn, S.K. Chang, Org. Lett. 10 (2008) 3717.
[3] M. Yuan, Y. Li, J. Li, C. Li, X. Liu, J. Xu, H. Liu, S. Wang, D. Zhu, Org. Lett. 9 (2007) 2313.
[4] R. Rekha, A.K. Jyothish, D. Ramaiah, Org. Lett. 9 (2007) 121.
[5] A. Dhir, V. Bhalla, M. Kumar, Org. Lett. 10 (2008) 4891.
[6] X. Chen, S.W. Nam, M.J. Jou, Y. Kim, S.-J. Kim, S. Park, J. Yoon, Org. Lett. 10 (2008) 5235.
[7] A.P. de Silva, D.B. Fox, A.J.M. Huxley, Coord. Chem. Rev. 205 (2000) 41.
[8] A.X. Trautwein, Bioinorganic Chemistry, Wiley-VCH, Weinheim, Germany, 1997.
[9] J. Huang, Y. Xu, X. Qian, J. Org. Chem. 74 (2009) 2167.
[10] S. Pandey, M. Ali, A. Bishnoi, A. Azam, S. Pandey, H.M. Chawla, J. Fluoresc. 18 (2008) 533.
[11] S. Pandey, A. Azam, S. Pandey, H.M. Chawla, Org. Biomol. Chem. 7 (2009) 269.
[12] S. Pandey, R. Jyotsna, A. Azam, S. Pandey, H.M. Chawla, J. Solution Chem. 39 (2010) 107.

[13] A. Caballero, R. Martinez, V. Lloveras, I. Ratera, J. Vidal-Gancedo, K. Wurst, A. Tarraga, P. Molina, J. Veciana, J. Am. Chem. Soc. 127 (2005) 15666.
[14] H. Li, H. Yan, J. Phys. Chem. 113 (2009) 7526.
[15] J.S. Lee, M.S. Han, C.A. Mirkin, Angew. Chem., Int. Ed. 46 (2007) 4093.
[16] W. Shi, H. Ma, Chem. Commun. 16 (2008) 1856.
[17] X. Zhang, Y. Xiao, X. Qian, Angew. Chem., Int. Ed. 47 (2008) 8025.
[18] L. Prodi, F. Bolletta, M. Montalti, N. Zaccheroni, Coord. Chem. Rev. 205 (2000) 59.
[19] K. Rurack, Spectrochim. Acta, Part A 57 (2001) 2161.
[20] W.K. Jung, H.C. Koo, K.W. Kim, S. Shin, S.H. Kim, Y.H. Park, Appl. Environ. Microbiol. 74 (2008) 2171.
[21] P. Passaniti, M. Maestri, P. Ceroni, G. Bergamini, F. Vötgle, H. Fakhrnabavi, O. Lukin, Photochem. Photobiol. Sci. 6 (2007) 471.
[22] J.S. Melo, J. Pina, F. Pina, C. Lodeiro, A.J. Parola, M.T. Albelda, M.P. Clares, E. García-Espańa, Phys. Chem. 107 (2003) 11307.
[23] A.W. Czarnik, Acc. Chem. Res. 27 (1994) 302.
[24] A.W. Czarnik, Fluorescent Chemosensors for Ion and Molecule Recognition, American Chemical Society, Washington, DC, 1992.
[25] L. Fabbrizzi, A. Poggi, Chem. Soc. Rev. 24 (1995) 197.
[26] A. Bencini, M.A. Bernardo, A. Bianchi, E. Garcia-Espańa, C. Giorgi, S. Luís, F. Pina, B. Valtancoli, in: G.W. Gokel (Ed.), In Advances in Supramolecular Chemistry, Cerberus Press, Miami, FL, 2002, pp. 79–130.
[27] A.J. Parola, J.C. Lima, C. Lodeiro, F. Pina, in: M.N. Berberan-Santos (Ed.), In Fluorescence of Supermolecules, Polymers, and Nanosystems, Springer-Verlag, Berlin, 2008, pp. 117–149.
[28] D.D. Perrin, W.L.F. Armango, D.R. Perrin, Purification of Laboratory Chemicals, Pergamon, Oxford, UK, 1986.
[29] E.M. Nolan, M.E. Racine, S.J. Lippard, Inorg. Chem. 45 (2006) 2742.
[30] A. Wolfe, G.H. Shimer, T. Meehan, Biochemistry 26 (1987) 6392.
[31] M.N.K. Andreia, C.C. Nunes, K.T. Mahmudov, M. Haukka, T.C.O. Mac Leod, L.M.D.R.S. Martins, M.L. Kuznetsova, A.J.L. Pombeiro, Dalton Trans. 40 (2011) 2822.
[32] J. Marten, W. Seichter, E. Weber, Z. Anorg. Allg. Chem. 631 (2005) 869.
[33] R. Pütter, Methoden Org. Chem. (Houben-Weyl) 10 (1965) 1.
[34] S. Sen, S. Mitra, P. Kundu, M.K. Saha, C. Krüger, J. Bruckmann, Polyhedron 16 (1997) 2475.
[35] G.M. Sheldrick, SHELXS-97 Program for the Solution of Crystal Structures, University of Göttingen, Göttingen, Germany, 1997.
[36] G.M. Sheldrick, Acta Crystallogr., Sect. A 46 (1990) 467.
[37] I.J. Bruno, J.C. Cole, P.R. Edgington, M. Kessler, C.F. Macrae, P. McCabe, J. Pearson, R. Taylor, Acta Crystallogr., Sect. B 58 (2002) 389.
[38] A.L. Spek, J. Appl. Crystallogr. 36 (2003) 7.
[39] H.-F. Li, P.-F. Yan, P. Chen, Y. Wang, H. Xu, G.-M. Li, Dalton Trans. 41 (2012) 900.
[40] P. Gilli, L. Pretto, V. Bertolasi, G. Gilli, Acc. Chem. Res. 42 (2009) 33.
[41] P. Simunek, V. Bertolasi, V. Machacek, J. Mol. Struct. 642 (2002) 41.
[42] P. Gilli, V. Bertolasi, L. Pretto, A. Lycka, G. Gilli, J. Am. Chem. Soc. 124 (2002) 13554.
[43] P. Gilli, V. Bertolasi, L. Pretto, G. Gilli, J. Mol. Struct. 790 (2006) 40.
[44] P. Sanz, O. Mo, M. Yanez, J. Elguero, Chem. Eur. J. 14 (2008) 4225.
[45] S.H. Lee, J.Y. Kim, S.K. Kim, J.H. Lee, J.S. Kim, Tetrahedron 60 (2004) 5171.
[46] Y. Saito, S. Miyamoto, A. Suzuki, K. Matsumoto, T. Ishihara, I. Saito, Bioorg. Med. Chem. Lett. 22 (2012) 2753.
[47] G.A. Jeffrey, An Introduction of Hydrogen Bonding, Oxford University Press, New York, Oxford, 1997.
[48] K.A. Connors, Binding Constants, Wiley, New York, 1987.
[49] H.J. Schneider, A. Yatsimirsky, Principles and Methods in Supramolecular Chemistry, Wiley, Chichester, UK, 2000.